

Solubility of the Single Gases Carbon Dioxide and Hydrogen in the Ionic Liquid [bmpy][Tf₂N]

Jacek Kumelań, Dirk Tuma, Álvaro Pérez-Salado Kamps, and Gerd Maurer*

Department of Mechanical and Process Engineering, University of Kaiserslautern, P.O. Box 3049, D-67653 Kaiserslautern, Germany

Experimental data for the solubility of the two single gases carbon dioxide and hydrogen in the ionic liquid 1-*n*-butyl-1-methylpyrrolidinium bis(trifluoromethylsulfonyl)amide ([bmpy][Tf₂N]) are reported for temperatures between (293.1 and 413.2) K. The maximum pressure (the maximum gas molality in the solvent) was 10.8 MPa (4.43 mol·kg⁻¹) for carbon dioxide and 8.9 MPa (0.14 mol·kg⁻¹) for hydrogen. The experiments were performed using a high-pressure view-cell technique operating on the synthetic method. The solubility of carbon dioxide in [bmpy][Tf₂N] is more than 1 order of magnitude higher than the solubility of hydrogen. Carbon dioxide becomes less soluble in [bmpy][Tf₂N] with increasing temperature, whereas hydrogen shows the opposite effect. An extension of Henry's law is employed to correlate the solubility pressures. The final results for the Henry's constant (at zero pressure) of carbon dioxide and hydrogen in [bmpy][Tf₂N] (on the molality scale) are represented within the experimental uncertainty (about 0.8 % for carbon dioxide and 1.3 % for hydrogen) by $\ln(k_{\text{H,CO}_2}^{(0)}/\text{MPa}) = 8.5128 - 2057/(T/\text{K}) - 0.004274 \cdot (T/\text{K})$ and $\ln(k_{\text{H,H}_2}^{(0)}/\text{MPa}) = 3.5746 + 343/(T/\text{K}) - 0.0008 \cdot (T/\text{K})$, respectively.

Introduction

A fundamental question in the assessment of the feasibility of applications involving ionic liquids and gases is to understand the structure–property relationship of the system ionic liquid + gas. Different from molecular solvents and unique for ionic liquids, the cation, the anion, and substituents on both the cation and anion can be tailored to enhance or suppress the solubility of a certain gas in that ionic liquid. Several research groups have already addressed the question whether the anion or the cation plays the most significant role in determining the gas solubilities.^{1–5} The results from their systematic studies confirm that the choice of the anion affects the solubility behavior most, whereas the effect from changing the cation is less significant but still noticeable.

In the course of our previous studies on gas solubility in ionic liquids, the solubility of seven different gases in the imidazolium-based ionic liquid 1-*n*-hexyl-3-methylimidazolium bis(trifluoromethylsulfonyl)amide ([hmim][Tf₂N]) was investigated between (293 and 413) K and up to higher pressures of approximately 10 MPa using a high-pressure view cell that operates according to the synthetic method.^{6–10} Apart from the two highly soluble gases carbon dioxide⁶ and xenon,⁸ five other gases which exhibit a particularly low solubility were studied. Those gases were, in order of decreasing solubility determined in our experiments, methane,⁸ oxygen,¹⁰ carbon monoxide,¹⁰ tetrafluoromethane,⁹ and ultimately hydrogen.⁷

For the present work, we resorted to another ionic liquid with the [Tf₂N]⁻ anion, the pyrrolidinium-substituted 1-*n*-butyl-1-methylpyrrolidinium bis(trifluoromethylsulfonyl)amide ([bmpy][Tf₂N]), which also was subject to the studies by the above-mentioned groups.^{1,3} New experimental data for the solubility of carbon dioxide (a high-soluble gas) as well as hydrogen (hydrogen always turned out to be the least soluble gas when

referring to the results of our previous studies)^{6–10} are presented. Solubility isotherms were recorded at temperatures from about (293 to 413) K in intervals of 40 K and up to 10 MPa. The maximum pressure (the maximum gas molality) amounts to 10.8 MPa (4.43 mol·kg⁻¹) for carbon dioxide and 8.9 MPa (0.14 mol·kg⁻¹) for hydrogen. The corresponding Henry's law constant of the gas was determined employing an extension of Henry's law.^{6–10} Additionally, the obtained results are compared with available literature data as well as with our results for the imidazolium-based ionic liquid [hmim][Tf₂N].

Experimental Section and Results

Apparatus and Method. The gas solubility apparatus and the experimental procedures were the same as for the corresponding investigations employing [hmim][Tf₂N].^{6,7} Therefore, only the workflow is sketched and amended with the specific differences that result from the systems investigated in the present study. For more details, the reader is referred, for example, to some references cited in the above-mentioned papers^{6,7} as well as to the book chapter by Maurer and Pérez-Salado Kamps¹¹ where a scheme of the apparatus is also provided.

Basically, the procedure consists of measuring the pressure required to dissolve a precisely known amount of gas in an also precisely known amount of solvent that fills a high-pressure view cell. Except for three data points at the highest gas molality for carbon dioxide, namely, two points of the isotherm at 333.1 K and a single point at 373.2 K, that were introduced via a condenser and thus determined gravimetrically, the mass of the gas introduced into the cell was determined volumetrically, i.e., from the known volume of the cell (approximately 29.2 cm³) and the density, which was calculated from readings for temperature and pressure via the software package “ThermoFluids”¹² for carbon dioxide and the virial equation of state that was truncated after the second virial coefficient for hydrogen.¹³ The calculations for carbon dioxide resorted to the approved equation of state developed by Span and Wagner.¹⁴ Gravimetric uncertainties amount to ± 0.01 g,

* Corresponding author. Tel.: +49 631 205 2410. Fax: +49 631 205 3835. E-mail: gerd.maurer@mv.uni-kl.de.

Table 1. Density of the Ionic Liquid [bmpy][Tf₂N] (Experimental Uncertainties: $\Delta T = \pm 0.1$ K; $\Delta \rho = \pm 0.0001$ kg·dm⁻³)

<i>T</i> /K	ρ /(kg·dm ⁻³)
289.0	1.4043
291.0	1.4026
293.0	1.4010
295.0	1.3994
297.05	1.3978
299.05	1.3962
301.05	1.3946
303.1	1.3931
305.1	1.3915
307.1	1.3900
309.1	1.3885

The amount of mass of the solvent (i.e., the ionic liquid [bmpy][Tf₂N]) filled into the cell was calculated from the volume displacement in a calibrated spindle press, which is used for the displacement of the solvent, and the solvent density. The density of the ionic liquid [bmpy][Tf₂N] was independently determined in the temperature region between (289.0 and 309.1) K using a vibrating tube densimeter (DMA 602, Anton Paar GmbH, Graz, Austria). These results are given in Table 1.

The temperature was measured using two calibrated platinum resistance thermometers with an uncertainty of less than ± 0.1 K. When the cell was charged with carbon dioxide, the pressure was recorded with two pressure transducers suitable for a maximum pressure of (2.5 and 6) MPa; in the experiments with hydrogen, two pressure transducers suitable for a maximum pressure of (0.25 and 0.6) MPa were employed. The corresponding solubility pressure was measured during both series with two pressure transducers suitable up to (2.5 and 10) MPa. Only the single measurement for carbon dioxide at 333.1 K resulting in a solubility pressure of 10.8 MPa required a pressure transducer that can operate up to 25 MPa. All pressure transducers were from WIKA GmbH, Klingenberg, Germany. They were calibrated against a high-precision pressure balance (Desgranges & Huot, Aubervilliers, France) before and after each measurement series. The maximum systematic uncertainty in the solubility pressure measurement results from the intrinsic

uncertainty of the pressure transducers (i.e., 0.1 % of the transducer's full scale) and an additional contribution of ± 0.01 MPa (± 0.015 MPa) for carbon dioxide (hydrogen). This additional contribution arises from a small temperature drift inside the isolated (high-pressure) tubes filled with the solvent, which connect the view cell with the pressure transducers. Several test runs verified that particular drift.

Materials and Sample Pretreatment. Carbon dioxide (4.5, mole fraction ≥ 0.99995) and hydrogen (5.0, mole fraction ≥ 0.99999) were from Messer Griesheim GmbH, Krefeld, Germany. Both gases were used without further purification. The ionic liquid [bmpy][Tf₂N] (C₁₁H₂₀N₂F₆O₄S₂, high purity, mass fraction ≥ 0.99 , colorless liquid, relative molar mass $M = 422.41$) was purchased from Merck KGaA, Darmstadt, Germany. Initially, the samples were degassed and dried under vacuum over a period of two days to remove traces of water and other volatile impurities. ¹H, ¹³C, and ¹⁹F NMR spectroscopic investigations were carried out with a Bruker Avance 600 MHz spectrometer (Bruker AXS GmbH, Karlsruhe, Germany), proving that the impurities of that sample were below 0.01 mol fraction. The mass fraction of water in the sample was less than 0.00023, as determined by Karl Fischer titration analysis after the completion of the measurement series. A glass buret served as a sample container, so that the ionic liquid could be handled and introduced into the apparatus always under vacuum, and any moisture from the laboratory air was blocked. The ionic liquid was collected after each measurement and reconditioned (i.e., degassed and dried under vacuum) for further use. No degradation was observed for [bmpy][Tf₂N] during the experiments with both gases, and NMR measurements of samples that had been collected from a measurement at 413 K did not give different results in comparison with raw samples.

Experimental Results. Gas solubilities were determined at four temperatures (of about (293, 333, 373, and 413) K) at pressures up to approximately 10 MPa. The corresponding solubility data are given in Table 2 (for carbon dioxide) and Table 3 (for hydrogen) as the pressure p that is required to dissolve the given amount of the gas in 1 kg of the ionic liquid

Table 2. Experimental Results for the Solubility of Gas G = Carbon Dioxide in [bmpy][Tf₂N]

<i>T</i> K	m_G (mol·kg ⁻¹)	<i>p</i> MPa	f_G/m_G MPa/(mol·kg ⁻¹)	V/\bar{m}_{HL} (cm ³ ·kg ⁻¹)
293.1 ± 0.1	0.2209 ± 0.0021	0.280 ± 0.015	1.249 ± 0.057	723.8 ± 2.3
	0.9469 ± 0.0058	1.147 ± 0.027	1.139 ± 0.021	753.7 ± 2.4
	1.1944 ± 0.0063	1.429 ± 0.028	1.107 ± 0.017	762.4 ± 2.4
	1.4784 ± 0.0069	1.741 ± 0.029	1.071 ± 0.013	774.5 ± 2.5
	1.7994 ± 0.0078	2.081 ± 0.030	1.032 ± 0.011	787.2 ± 2.5
	2.5122 ± 0.0097	2.807 ± 0.032	0.955 ± 0.008	808.8 ± 2.6
	3.7590 ± 0.0199	3.899 ± 0.045	0.829 ± 0.006	864.5 ± 2.9
	0.4691 ± 0.0017	1.163 ± 0.017	2.382 ± 0.027	754.9 ± 2.4
333.1 ± 0.1	0.7121 ± 0.0024	1.758 ± 0.018	2.322 ± 0.018	764.5 ± 2.4
	1.1408 ± 0.0041	2.788 ± 0.030	2.215 ± 0.018	782.2 ± 2.5
	1.6609 ± 0.0057	4.010 ± 0.034	2.092 ± 0.013	803.1 ± 2.6
	2.2630 ± 0.0076	5.398 ± 0.039	1.960 ± 0.010	828.9 ± 2.7
	3.1107 ± 0.0110	7.258 ± 0.048	1.780 ± 0.008	861.7 ± 2.8
	4.4339 ± 0.0135	10.813 ± 0.069	1.593 ± 0.007	915.7 ± 3.0
	0.3917 ± 0.0014	1.594 ± 0.018	3.921 ± 0.034	770.9 ± 2.4
	0.5722 ± 0.0019	2.359 ± 0.020	3.900 ± 0.025	778.6 ± 2.5
373.2 ± 0.1	0.9573 ± 0.0035	3.924 ± 0.034	3.737 ± 0.023	795.7 ± 2.5
	1.3415 ± 0.0046	5.505 ± 0.039	3.602 ± 0.018	810.7 ± 2.6
	1.7820 ± 0.0060	7.322 ± 0.045	3.450 ± 0.015	829.5 ± 2.7
	2.3670 ± 0.0100	9.718 ± 0.061	3.250 ± 0.015	852.3 ± 2.8
	0.3270 ± 0.0012	1.934 ± 0.019	5.733 ± 0.043	786.8 ± 2.5
	0.6184 ± 0.0021	3.665 ± 0.032	5.588 ± 0.036	799.6 ± 2.5
	0.8489 ± 0.0031	5.047 ± 0.038	5.483 ± 0.029	809.2 ± 2.6
	1.0991 ± 0.0038	6.553 ± 0.042	5.368 ± 0.025	820.3 ± 2.6
413.2 ± 0.1	1.3635 ± 0.0046	8.160 ± 0.047	5.252 ± 0.022	832.5 ± 2.7
	1.6460 ± 0.0055	9.916 ± 0.052	5.143 ± 0.020	844.8 ± 2.7

Table 3. Experimental Results for the Solubility of Gas G = Hydrogen in [bmpy][Tf₂N]

T	m_G	p	f_G/m_G	V/\bar{m}_{HL}
K	(mol·kg ⁻¹)	MPa	MPa/(mol·kg ⁻¹)	(cm ³ ·kg ⁻¹)
293.2 ± 0.1	0.01622 ± 0.00009	1.472 ± 0.026	91.6 ± 1.2	713.7 ± 2.2
	0.03101 ± 0.00012	2.859 ± 0.036	93.7 ± 0.9	713.4 ± 2.2
	0.05189 ± 0.00018	4.772 ± 0.041	94.6 ± 0.6	712.6 ± 2.2
	0.07175 ± 0.00024	6.639 ± 0.047	96.2 ± 0.5	712.7 ± 2.2
	0.08450 ± 0.00032	7.834 ± 0.054	97.1 ± 0.5	712.4 ± 2.2
	0.09612 ± 0.00035	8.945 ± 0.057	98.1 ± 0.4	713.1 ± 2.2
333.1 ± 0.1	0.01866 ± 0.00009	1.443 ± 0.024	78.0 ± 1.0	732.0 ± 2.3
	0.03649 ± 0.00013	2.826 ± 0.035	78.6 ± 0.7	732.2 ± 2.3
	0.05189 ± 0.00018	4.032 ± 0.039	79.4 ± 0.6	731.4 ± 2.3
	0.06762 ± 0.00022	5.240 ± 0.042	79.7 ± 0.5	732.0 ± 2.3
	0.08768 ± 0.00032	6.889 ± 0.049	81.6 ± 0.4	731.3 ± 2.3
	0.10679 ± 0.00037	8.408 ± 0.054	82.4 ± 0.4	731.0 ± 2.3
373.1 ± 0.1	0.02086 ± 0.00009	1.384 ± 0.023	66.8 ± 0.9	750.6 ± 2.4
	0.04051 ± 0.00014	2.707 ± 0.034	67.8 ± 0.7	750.9 ± 2.4
	0.06041 ± 0.00020	4.038 ± 0.038	68.2 ± 0.5	750.1 ± 2.4
	0.08150 ± 0.00030	5.465 ± 0.045	68.9 ± 0.4	750.6 ± 2.4
	0.10251 ± 0.00035	6.913 ± 0.048	69.8 ± 0.3	750.3 ± 2.4
	0.12337 ± 0.00042	8.325 ± 0.052	70.4 ± 0.3	750.6 ± 2.4
413.2 ± 0.1	0.02312 ± 0.00009	1.365 ± 0.023	59.4 ± 0.8	769.4 ± 2.4
	0.04581 ± 0.00016	2.708 ± 0.034	59.9 ± 0.6	769.2 ± 2.4
	0.06721 ± 0.00025	3.955 ± 0.040	59.9 ± 0.4	769.6 ± 2.4
	0.09399 ± 0.00033	5.517 ± 0.044	60.2 ± 0.3	769.7 ± 2.4
	0.11773 ± 0.00040	6.972 ± 0.048	61.2 ± 0.3	769.5 ± 2.4
	0.13939 ± 0.00046	8.272 ± 0.052	61.7 ± 0.3	769.9 ± 2.4

at a fixed temperature. In Figure 1, the solubility pressure p is plotted versus the gas molality m_G [i.e., the amount of substance (the number of moles) of the gas per kilogram of [bmpy][Tf₂N]] at constant temperature T (left diagram for carbon dioxide, right diagram for hydrogen).

For both gases and within the temperature and pressure regions investigated during this study, the solubility pressure monotonously increases with increasing gas molality at a given temperature. As can also be seen in Figure 1, the solubility isotherms of carbon dioxide develop a minor curvature toward increasing pressures, whereas the solubility isotherms of hydrogen run almost linearly. This is typical for a purely physical solubility behavior and in accordance with our findings from investigations on gas solubility of carbon dioxide and hydrogen in other ionic liquids.^{6,7,15–17} In the same way, carbon dioxide and hydrogen show an opposite solubility behavior with increasing temperature (and constant pressure); higher temperatures lead to lower solubilities of carbon dioxide but higher solubilities of hydrogen. The temperature-induced solubility shift

in either direction remains distinct for both gases and is only slightly weakened at higher temperatures. Under equal conditions, the solubility of hydrogen in [bmpy][Tf₂N] is between about 1 and 2 orders of magnitude lower than the solubility of carbon dioxide. To give an example, at $p = 3.5$ MPa and $T = 293$ K (413 K), about 3.3 (0.59) moles of carbon dioxide {0.038 (0.059) moles of hydrogen} dissolve in 1 kg of [bmpy][Tf₂N].

The experimental uncertainty for the gas molality Δm_G (caused by the filling procedure) was estimated from a Gauss error propagation calculation and amounts at average to 0.0059 mol·kg⁻¹ (0.41 %) for the system (carbon dioxide + [bmpy][Tf₂N]) and to 0.00024 mol·kg⁻¹ (0.37 %) for the system (hydrogen + [bmpy][Tf₂N]). From previous studies (see, e.g., ref 9), it was proven reasonable to estimate the experimental uncertainty for the solubility pressure p as the sum of two contributions: $\Delta p = \pm (\Delta p_{\text{sys}} + \Delta p_{\text{stat}})$. The first term accounts for the systematic uncertainties [i.e., pressure transducer's uncertainty (0.1 % of the transducer's full scale) + uncertainty resulting from the temperature drift (0.01 MPa for carbon

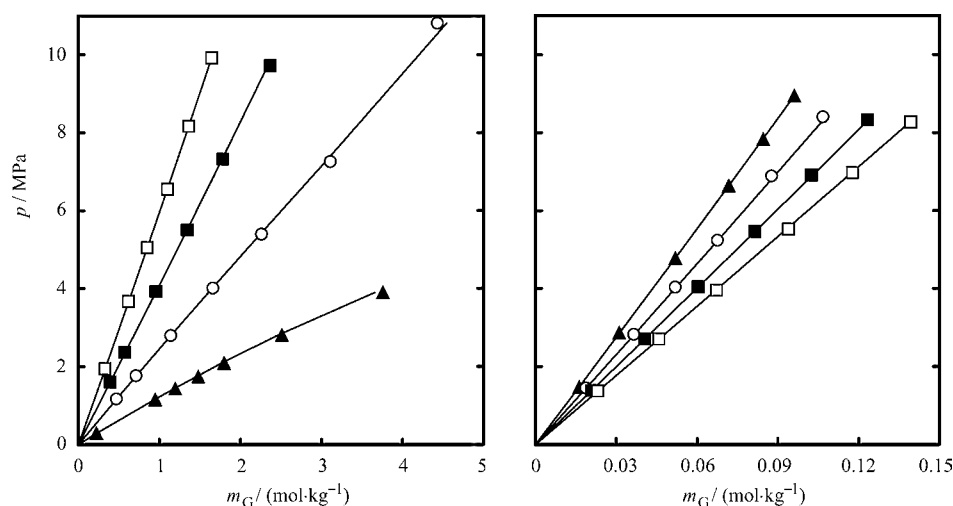


Figure 1. Total pressure above solutions of (gas G + [bmpy][Tf₂N]): left diagram, G is CO₂; right diagram, G is H₂; (▲, ~293 K; ○, ~333 K; ■, ~373 K; □, ~413 K) experimental results; —, correlation.

dioxide and 0.015 MPa for hydrogen)}. The second term is a statistical one from a Gauss error propagation calculation (by applying the vapor–liquid equilibrium model described in the next section). It reflects the effect of the uncertainties of temperature and gas molality on the solubility pressure p . The absolute (relative) uncertainty in the pressure Δp ($\Delta p/p$) amounts in average to about 0.019 MPa (0.8 %) for the system (carbon dioxide + [bmpy][Tf₂N]) and to about 0.041 MPa (1.0 %) for the system (hydrogen + [bmpy][Tf₂N]). For carbon dioxide, the relative uncertainty decreases from at maximum 1.7 % (a single measurement at 293.1 K resulted in an exceptionally low solubility pressure of 0.280 MPa that is afflicted by a significantly higher relative uncertainty of 4.5 %) at low pressures to (at minimum) 0.2 % at the highest pressure. For hydrogen, this relative uncertainty decreases from at maximum 1.7 % at low pressures to (at minimum) 0.6 % at the highest pressure.

Correlation of Gas Solubility

The correlation method applied here is basically equal to that applied in our previous work on the solubility of carbon dioxide and hydrogen in other ionic liquids.^{6,7,15–18} To guide the reader, the framework with the main assumptions is repeated. The vapor pressure of the ionic liquid [bmpy][Tf₂N] is assumed to be very low and similar to that of, for example, [hmim][Tf₂N].¹⁹ Thus, it is neglected, and the gaseous phase is assumed to completely consist of the pure gas component. Consequently, the vapor–liquid equilibrium condition is only applied to that gas component. It results in the extended Henry's law

$$k_{H,G}(T, p) \cdot a_G(T, m_G) = f_G(T, p) \quad (1)$$

$k_{H,G}(T, p)$ is Henry's constant of gas G in [bmpy][Tf₂N] at temperature T and pressure p (based on the molality scale). $a_G(T, m_G)$ is the activity of the gas in the liquid phase at temperature T and gas molality m_G . The influence of pressure on that activity is neglected. $f_G(T, p)$ is the fugacity of the gas in the vapor phase.

The influence of pressure on Henry's constant is expressed as

$$k_{H,G}(T, p) = k_{H,G}^{(0)}(T) \cdot \exp\left(\frac{V_{m,G}^{(\infty)} \cdot p}{R \cdot T}\right) \quad (2)$$

where $k_{H,G}^{(0)}(T)$ is the Henry's constant at zero pressure; $V_{m,G}^{(\infty)}$ is the partial molar volume of the gas at infinite dilution in the ionic liquid; and R is the universal gas constant.

The activity of the respective gas in the ionic liquid (on the molality scale) is

$$a_G = \frac{m_G}{m^\circ} \cdot \gamma_G \quad (3)$$

where $m^\circ = 1 \text{ mol} \cdot \text{kg}^{-1}$. The activity coefficient γ_G is calculated employing the virial expansion for the excess Gibbs energy (also on the molality scale) according to Pitzer^{20,21}

$$\ln \gamma_G = 2 \cdot \frac{m_G}{m^\circ} \cdot \beta_{G,G}^{(0)} + 3 \cdot \left(\frac{m_G}{m^\circ}\right)^2 \cdot \mu_{G,G,G} \quad (4)$$

The parameters $\beta_{G,G}^{(0)}$ and $\mu_{G,G,G}$ of eq 4 describe binary and ternary interactions, respectively, between gas molecules in the solvent.

Ultimately, the fugacity of the pure gas f_G at equilibrium temperature and pressure is the product of the total pressure p and the fugacity coefficient $\phi_G(T, p)$

$$f_G(T, p) = p \cdot \phi_G(T, p) \quad (5)$$

In this study, the fugacity coefficients $\phi_G(T, p)$ of G = carbon dioxide were calculated employing "ThermoFluids",¹² but those of G = hydrogen were calculated via the virial equation of state, truncated after the second virial coefficient.

$$\phi_G(T, p) = \exp\left[\frac{B_{G,G} \cdot p}{R \cdot T}\right] \quad (6)$$

The second virial coefficient of hydrogen B_{H_2, H_2} was calculated from a correlation⁷ which is based on experimental data recommended by Hayden and O'Connell.¹³

An extrapolation (with the temperature set constant) of the experimental results for the solubility pressure of the respective gas in [bmpy][Tf₂N] gives Henry's constant of the gas in [bmpy][Tf₂N] at zero pressure $k_{H,G}^{(0)}(T)$

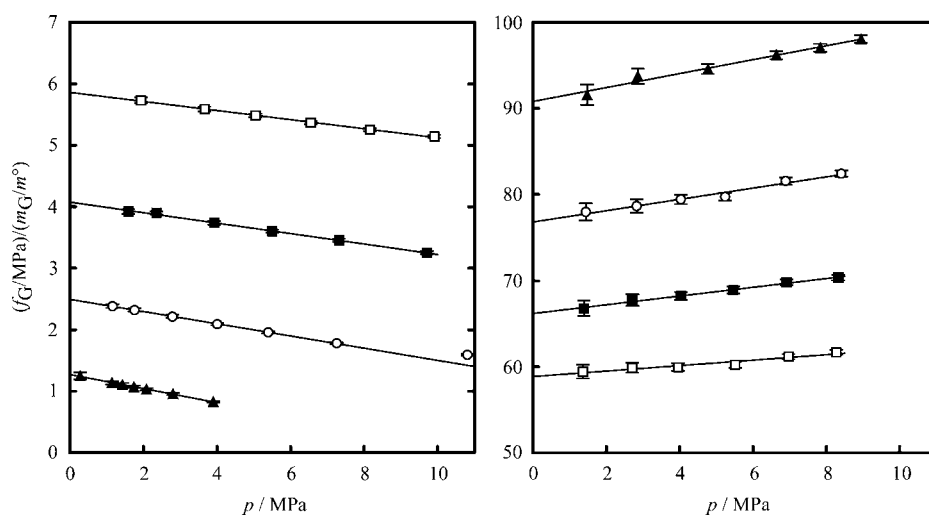


Figure 2. Influence of the total pressure on the ratio of the fugacity of gas G (in the gaseous phase) to the molality of that gas (in the ionic liquid [bmpy][Tf₂N]): left diagram, G is CO₂; right diagram, G is H₂; (▲, ~293 K; ○, ~333 K; ■, ~373 K; □, ~413 K) experimental results and estimated uncertainties; —, linear fit.

$$k_{H,G}^{(0)}(T) = \lim_{p \rightarrow 0} \left[\frac{f_G(T,p)}{m_G/m^\circ} \right] \quad (7)$$

The results for $f_G/(m_G/m^\circ)$ together with the estimated uncertainties from a Gauss error propagation calculation are also given in Tables 2 and 3, and Figure 2 shows the extrapolation to zero pressure for carbon dioxide and hydrogen, respectively. $k_{H,G}^{(0)}(T)$ is determined from a linear regression. This extrapolation was repeated omitting randomly selected single or double data points to ensure that the number of experimental points used for the extrapolation does not have an influence on the final result for Henry's constant. The given uncertainty $\Delta(f_G/(m_G/m^\circ))$ is the deviation between the optimum value (i.e., obtained from all data) and the result of the above-mentioned procedure (i.e., selected data omitted). Table 4 lists the numerical results for Henry's constant (at zero pressure and on the molality scale) after applying this procedure.

The estimated relative uncertainty for those Henry's constants amounts in average to 0.8 % for carbon dioxide and to 1.3 % for hydrogen.

$$\ln(k_{H,CO_2}^{(0)}/\text{MPa}) = 8.5128 - 2057/(T/K) - 0.004274 \cdot (T/K) \quad (8)$$

$$\ln(k_{H,H_2}^{(0)}/\text{MPa}) = 3.5746 + 343/(T/K) - 0.0008 \cdot (T/K) \quad (9)$$

Equations 8 and 9 describe Henry's constant as a function of temperature. The deviation between experimental and correlated values for Henry's constant remains within the experimental uncertainty given in Table 4. In Figure 3, both the data obtained from extrapolation to zero pressure and the correlation function for Henry's constant (cf. eqs 8 and 9) are plotted versus the inverse absolute temperature. The figure also shows the opposite solubility behavior of carbon dioxide and hydrogen.

In general, the correlation of the solubility pressure resorts to results for the Henry's constant, the partial molar volume of the respective gas infinitely diluted in the ionic liquid [bmpy][Tf₂N] $V_{m,G}^{(\infty)}$, and the interaction parameters $\beta_{G,G}^{(0)}$ and

Table 4. Henry's Constant of the Gas G in [bmpy][Tf₂N] (at Zero Pressure, on the Molality Scale)

gas G	T/K	$k_{H,G}^{(0)}/\text{MPa}$
carbon dioxide	293.1	1.274 ± 0.019
	333.1	2.496 ± 0.014
	373.2	4.075 ± 0.022
	413.2	5.864 ± 0.029
hydrogen	293.2	90.8 ± 1.2
	333.1	76.8 ± 1.0
	373.1	66.2 ± 0.9
	413.2	58.9 ± 0.8

Table 5. Experimental Results for the Specific Volume v_{IL} of the Pure Ionic Liquid [bmpy][Tf₂N] and the Partial Molar Volume of Carbon Dioxide and Hydrogen at Infinite Dilution $V_{m,G}^{(\infty)}$ in [bmpy][Tf₂N]

gas G	T/K	$V_{m,G}^{(\infty)}/(\text{cm}^3 \cdot \text{mol}^{-1})$		$v_{IL}/(\text{cm}^3 \cdot \text{kg}^{-1})$
		from gas solubility data (i.e., $\beta_{G,G}^{(0)} = \mu_{G,G,G}^{(0)} = 0$)	from volumetric data	from volumetric data
carbon dioxide	293.1	—	38.9 ± 1.0	715.7 ± 2.5
	333.1	—	40.5 ± 1.0	735.9 ± 2.7
	373.2	—	42.1 ± 1.5	755.2 ± 2.6
	413.2	—	43.7 ± 2.0	772.2 ± 2.6
hydrogen	293.2	21 ± 10	—	713.0 ± 2.2
	333.1	21 ± 10	—	731.7 ± 2.3
	373.1	21 ± 10	—	750.5 ± 2.3
	413.2	21 ± 10	—	769.6 ± 2.4

$\mu_{G,G,G}$. The curves in Figure 1 represent the correlation results for the solubility pressure.

The applied measuring technique in principle enables us to determine the partial molar volume at infinite dilution. Data evaluation, which resorts to so-called volumetric properties, of various different systems (gas + ionic liquid) proved necessary to distinguish between highly and poorly soluble gases and to execute different methods accordingly.²² In this regard, carbon dioxide clearly belongs to the category of highly soluble gases and hydrogen to that of poorly soluble gases. Figure 4 shows a plot (V/\tilde{m}_{IL}) versus the corresponding gas molalities m_G for both gases at a constant temperature. V stands for the volume of the view cell, i.e., the volume of the equilibrated liquid mixture in that cell, and \tilde{m}_{IL} is the mass of the ionic liquid in that liquid mixture. The (V/\tilde{m}_{IL}) values together with their experimental uncertainty estimated from a Gauss error propagation calculation are listed in Table 2 and Table 3, respectively.

As demonstrated in detail in the above-mentioned previous paper,²² according to eq 10, the slope of the linear functions associated with the data shown in Figure 4 represents the partial molar volume of the dissolved gas at infinite dilution $V_{m,G}^{(\infty)}$. Additionally, the intercept of that linear function with the y-axis yields the specific volume v_{IL} of the pure solvent (i.e., the ionic liquid [bmpy][Tf₂N]).

$$\frac{V/\text{cm}^3}{\tilde{m}_{IL}/\text{g}} = v_{IL}/(\text{cm}^3 \cdot \text{g}^{-1}) + \frac{m_G}{1000m^\circ} \cdot V_{m,G}^{(\infty)}/(\text{cm}^3 \cdot \text{mol}^{-1}) \quad (10)$$

This value, however, should not make up for a density measurement of the pure solvent by, for example, a vibrating-tube densimeter because of its minor accuracy²² but can be taken for verification. At 293.0 K, the v_{IL} value from densimeter measurements (cf. Table 1) amounts to (713.77 ± 0.06) $\text{cm}^3 \cdot \text{kg}^{-1}$, which is embedded within the error margin of both corresponding values that were obtained from volumetric data (cf. Table 5).

For carbon dioxide, due to the high solubility in the ionic liquid [bmpy][Tf₂N], $V_{m,CO_2}^{(\infty)}$ can be evaluated from a linear regression of the experimentally determined volumetric data with appropriate accuracy. To do so, the value for v_{IL} , which results from a fit of the independently determined density values (cf. Table 1), was taken to anchor the linear function at $T = 293.1$ K (see Figure 4); the values for v_{IL} for the other temperatures (i.e., at $T = (333.1, 373.2, \text{ and } 413.2)$ K and thus beyond the temperature range investigated by the densimeter) resulted from the linear fit to the volumetric data. The influence of temperature on $V_{m,CO_2}^{(\infty)}$ was then as well described by a linear function. Then, the interaction parameters $\beta_{CO_2,CO_2,CO_2}^{(0)}$ and μ_{CO_2,CO_2,CO_2} remain as unknown properties and were fit to the gas solubility data using Henry's constants and the partial molar volume at infinite dilution $V_{m,CO_2}^{(\infty)}$ from volumetric data.

$$V_{m,CO_2}^{(\infty)}/(\text{cm}^3 \cdot \text{mol}^{-1}) = 27.183 + 0.04 \cdot (T/K) \quad (11)$$

$$\beta_{CO_2,CO_2}^{(0)} = -0.1127 + 14.41/(T/K) \quad (12)$$

$$\mu_{CO_2,CO_2,CO_2} = 0 \quad (13)$$

In contrast, values for the partial molar volume $V_{m,H_2}^{(\infty)}$ of the poorly soluble hydrogen resulting from the volumetric data go with a significant uncertainty. We estimated the uncertainty from the evaluation of volumetric data of systems with gases that show poor solubility to about $10 \text{ cm}^3 \cdot \text{mol}^{-1}$.²² This high uncertainty is illustrated in Figure 4, where the volumetric data

for hydrogen show that even physically unrealistic results of both $V_{m,H_2}^{(\infty)} = 0$ and $V_{m,H_2}^{(\infty)} < 0$ fall within the experimental uncertainty. However, the low solubility also allows for the assumption of ideal mixing behavior ($\gamma_{H_2} = 1$), so that the partial molar volume at infinite dilution $V_{m,H_2}^{(\infty)}$ remains the only unknown property. It is therefore most reasonable to fit $V_{m,H_2}^{(\infty)}$ to the experimental solubility data.

For hydrogen, the following equations for the model parameters $V_{m,G}^{(\infty)}$, $\beta_{G,G}^{(0)}$, and $\mu_{G,G,G}$ were applied to correlate the gas solubility data.

$$V_{m,H_2}^{(\infty)}/(\text{cm}^3 \cdot \text{mol}^{-1}) = 21 \quad (14)$$

$$\beta_{H_2,H_2}^{(0)} = 0 \quad (15)$$

$$\mu_{H_2,H_2,H_2} = 0 \quad (16)$$

The results for the derived specific volume v_{IL} of the pure solvent and the partial molar volume at infinite dilution $V_{m,G}^{(\infty)}$ for the systems investigated in the present study are given in Table 5.

The correlation results for the gas solubility (i.e., the gas molalities at a given temperature and solubility pressure) agree with the data from the laboratory experiment within an average

absolute (relative) deviation of about $0.019 \text{ mol} \cdot \text{kg}^{-1}$ (0.82 %) for the system (carbon dioxide + [bmpy][Tf₂N]) and of about $0.0027 \text{ mol} \cdot \text{kg}^{-1}$ (0.40 %) for the system (hydrogen + [bmpy][Tf₂N]).

Additionally, the partial molar volume $V_{m,G}^{(\infty)}$ can also be employed to estimate the relative volume expansion of the liquid that is caused by the uptake of gas according to

$$\frac{\Delta V}{V} = \frac{m_G}{m^o} \cdot \frac{V_{m,G}^{(\infty)}/(\text{cm}^3 \cdot \text{mol}^{-1})}{v_{IL}/(\text{cm}^3 \cdot \text{kg}^{-1})} \quad (17)$$

At $p = 10 \text{ MPa}$, the volume expansion for carbon dioxide (hydrogen) amounts to 23 % (0.4 %) at 333 K and 9.4 % (0.5 %) at 413 K, respectively.

The knowledge of Henry's constant is necessary to calculate various related (molar) solution thermodynamic properties, $\Delta_{\text{sol}}X_m^o$, where, for example, X can be replaced by G (the Gibbs energy), H (the enthalpy), S (the entropy), or C_p (the heat capacity at constant pressure).¹⁵ Table 6 shows the resulting values at standard conditions ($T^o = 298.15 \text{ K}$, $p^o = 0.1 \text{ MPa}$) and on the molality scale which result from the correlation equations given above.

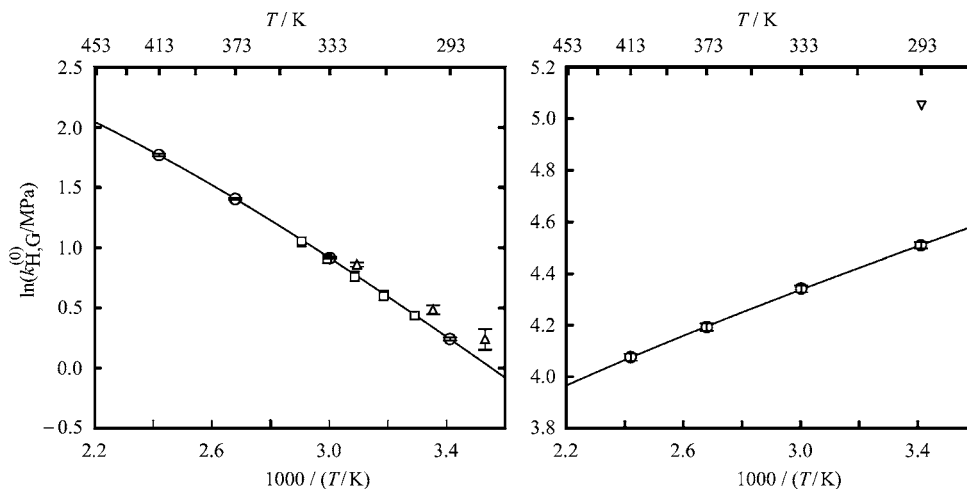


Figure 3. Henry's constant of gas G in [bmpy][Tf₂N] (at zero pressure, on the molality scale) plotted against the (inverse) temperature: left diagram, G is CO₂; right diagram, G is H₂; O, extrapolated experimental results and estimated uncertainties, this work; — correlation, this work; Δ, Anthony et al.¹ (including reported uncertainties); □, Hong et al.;³ ▽, Dyson et al.²³

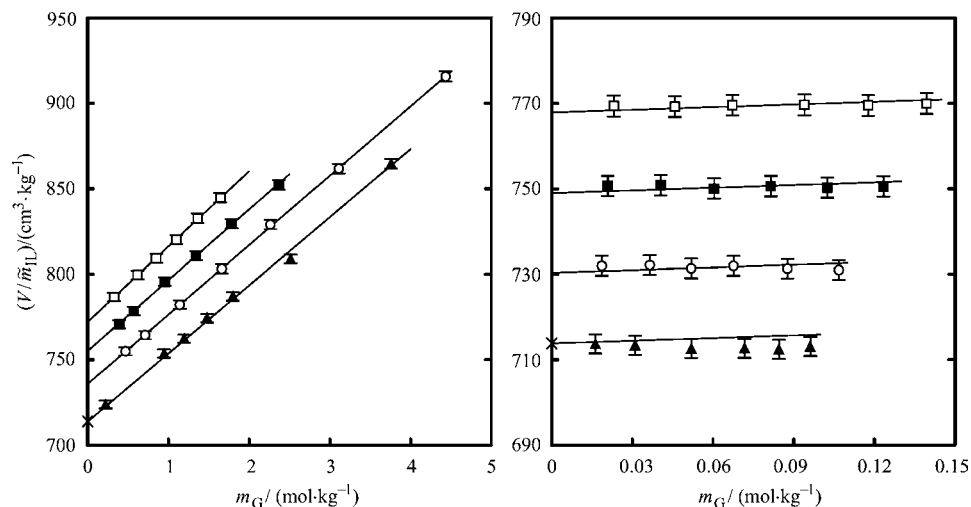


Figure 4. Volumetric data from the investigations of the system (gas G + [bmpy][Tf₂N]): left diagram, G is CO₂; right diagram, G is H₂; (▲, ~293 K; ○, ~333 K; ■, ~373 K; □, ~413 K) experimental results and estimated uncertainties; —, calculation results (linear function); ×, specific volume of the pure ionic liquid [bmpy][Tf₂N] as determined with a vibrating-tube densimeter (cf. Table 1).

Table 6. Results for the Molar Solution Properties $\Delta_{\text{sol}}X_m^0$ at Standard Conditions ($T^\circ = 298.15$ K, $p^\circ = 0.1$ MPa) and on the Molality Scale from Henry's Constant

$\Delta_{\text{sol}}X_m^0$	carbon dioxide	hydrogen
$\Delta_{\text{sol}}G_m^0/(\text{kJ}\cdot\text{mol}^{-1})$	6.553 ± 0.033	16.832 ± 0.033
$\Delta_{\text{sol}}H_m^0/(\text{kJ}\cdot\text{mol}^{-1})$	-13.94 ± 0.21	3.45 ± 0.18
$\Delta_{\text{sol}}S_m^0/(\text{J}\cdot\text{mol}^{-1}\cdot\text{K}^{-1})$	-68.74 ± 0.71	-44.90 ± 0.61
$\Delta_{\text{sol}}C_{p,m}^0/(\text{J}\cdot\text{mol}^{-1}\cdot\text{K}^{-1})$	21.2 ± 1.5	—

Discussion and Comparison with Literature Data

In Figure 5, Henry's constant (at zero pressure and on the molality scale) for carbon dioxide and hydrogen in the ionic liquids investigated by us so far (i.e., [bmim][CH₃SO₄], [bmim][PF₆], [bmpy][Tf₂N], and [hmim][Tf₂N]) are plotted versus the inverse temperature.

The curves represent correlation results only (cf. eqs 8 and 9 for [bmpy][Tf₂N]). All ionic liquids investigated feature a decreasing gas solubility with increasing temperature for carbon dioxide but an increasing gas solubility with increasing temperature for hydrogen.

Within the investigated temperature range, the (zero pressure) Henry's constant of carbon dioxide $k_{\text{H,CO}_2}^{(0)}$ in [bmim][CH₃SO₄] is distinctly higher compared to the other ionic liquids [bmim][PF₆], [bmpy][Tf₂N], and [hmim][Tf₂N]. The functions of $k_{\text{H,CO}_2}^{(0)}$ in these ionic liquids draw quite straight lines except for [bmim][PF₆], where a curvature toward lower values develops at lower temperatures. At 293 K, Henry's constant of carbon dioxide $k_{\text{H,CO}_2}^{(0)}$ is highest for [bmim][CH₃SO₄], followed by [bmpy][Tf₂N], [hmim][Tf₂N], and [bmim][PF₆] featuring the lowest value. At 413 K, this sequence is altered to [bmim][CH₃SO₄], then [bmim][PF₆], [bmpy][Tf₂N], and at last [hmim][Tf₂N]. The differences between the $k_{\text{H,CO}_2}^{(0)}$ values for [bmpy][Tf₂N] and the corresponding values for the other ionic liquids at 293 K (413 K) amount to -7 % ($+5$ %) for [bmim][PF₆], $+46$ % ($+45$ %) for [bmim][CH₃SO₄], and ultimately -3 % (-6 %) for [hmim][Tf₂N].

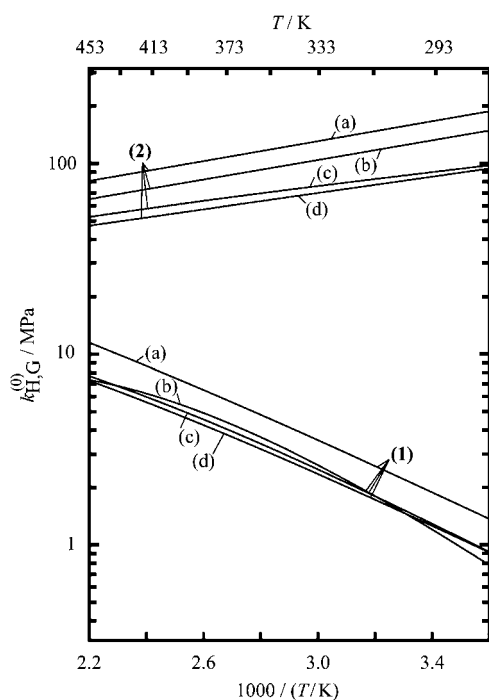


Figure 5. Correlation results for Henry's constant (at zero pressure, on the molality scale) of carbon dioxide (1) and hydrogen (2) in different ionic liquids: (a) [bmim][CH₃SO₄];^{16,17} (b) [bmim][PF₆];^{7,15,16} (c) [bmpy][Tf₂N], this work; (d) [hmim][Tf₂N].^{6,18}

Henry's constant of hydrogen $k_{\text{H,H}_2}^{(0)}$ in the examined ionic liquids shapes a more distinct behavior. Here, apart from the reverse temperature dependence, the functions show a plain and uniform sequence within the temperature range investigated, with the highest values for [bmim][CH₃SO₄], followed by [bmim][PF₆], [bmpy][Tf₂N], and ultimately [hmim][Tf₂N]. The differences between the $k_{\text{H,H}_2}^{(0)}$ values for [bmpy][Tf₂N] and the corresponding values for the other ionic liquids at 293 K (413 K) amount to $+47$ % ($+27$ %) for [bmim][PF₆], $+85$ % ($+58$ %) for [bmim][CH₃SO₄], and -5 % (-10 %) for [hmim][Tf₂N].

As far as [Tf₂N]⁻ ionic liquids are concerned, Hong et al.³ have studied the solubility of carbon dioxide and ethane in three different ionic liquids based on the [Tf₂N]⁻ anion at temperatures from (303 to 343) K and close to atmospheric pressure. Both gases appear as more (but not drastically more) soluble in the ionic liquid with the cyclic, nonaromatic cation 1-*n*-butyl-1-methylpyrrolidinium [bmpy]⁺ and less soluble in the compounds with the cation being an imidazolium (1-ethyl-3-methylimidazolium) or an ammonium (propylcholinium) derivative. A similar observation has also been made by Anthony et al.¹ for the carbon dioxide and oxygen solubility in another series of [Tf₂N]⁻ ionic liquids from measurements between (283 and 323) K and up to a maximum gas pressure of 1.3 MPa. Hou and Baltus⁴ also investigated carbon dioxide solubility in a series of [Tf₂N]⁻ ionic liquids at temperatures in the range between (283 and 323) K at pressures up to 8.4 MPa. They observed the carbon dioxide solubility following the trend: 1,2-dimethyl-3-propylimidazolium [pmmim] < 1-*n*-butyl-3-methylimidazolium [bmim] < 1-*n*-butyl-3-methylpyridinium < 1-(3,4,5,6-perfluoro-*n*-hexyl)-3-methylimidazolium [perfluoro-hmim]. Hou and Baltus⁴ explain the minor solubility by a reduced free volume available for CO₂, which an extra substituent or a shorter alkyl chain is responsible for. This sterically induced solubility behavior was observed by Aki et al.⁵ as well in a similar study. They investigated and compared, among others, the solubility of carbon dioxide in [bmim][Tf₂N], [hmim][Tf₂N], [omim][Tf₂N] ([omim] = 1-*n*-octyl-3-methylimidazolium), and the trisubstituted [hmmim][Tf₂N] ([hmmim] = 1-*n*-hexyl-2,3-dimethylimidazolium) at (25, 40, and 60) °C and to a maximum pressure of 15 MPa. In addition to this steric factor, both Hou and Baltus⁴ and Aki et al.⁵ look at molecular interactions. The ability of the cation to distribute and stabilize its charge was associated with the gas solubility. Stronger interactions between the dissolved gas molecule and the anion of the ionic liquid, accompanied by weaker cation-anion interactions and thus resulting in higher solubilities, are assigned to the nonaromatic pyridinium cation. The presence of large fluorine atoms also impacts the distribution of charges in addition to a steric influence, and that consequently influences the gas solubility.

In addition, one important result of the systematic study on the anion influence on gas solubility performed by Brennecke and co-workers⁵ was that the highest carbon dioxide solubility is found with anions containing fluoroalkyl groups (such as [Tf₂N]⁻) and the least solubility with nonfluorinated anions, whereas the two ionic liquids with inorganic fluorinated anions, [BF₄]⁻ and [PF₆]⁻, lie in between these two groups.

It can be seen in Figure 5 that the sequence of gas solubility agrees with these considerations.

The solubility of carbon dioxide in [bmpy][Tf₂N] was also investigated by the groups of Brennecke (Anthony et al.,¹ at (10, 25, and 50) °C and up to pressures of 1.3 MPa using a gravimetric microbalance) and Costa Gomes and Husson (Hong et al.,³ between (300 and 345) K at pressures close to atmospheric using an isochoric saturation method). Both report

Henry's constants in their papers; their results were converted to the molality scale and assembled together with our results in Figure 3 for comparison. The results for Henry's constant reported by Anthony et al.¹ are shifted to higher values compared to our data. Considering the reported uncertainty, the average relative deviation between the result from our correlation and the (minimum) reported value amounts to 11 % at best. The second data set from Hong et al.³ complies very well with our results, with the respective average relative deviation at 1.5 %.

In the case of hydrogen in [bmpy][Tf₂N], however, there is only one single point at 298 K available that was determined by Dyson et al.²³ using high-pressure ¹H NMR spectroscopy. That result (converted into the molality scale) is 76 % higher than the corresponding value from our experiment.

The molar solution properties at standard conditions (cf. Table 6) of carbon dioxide and hydrogen in [bmpy][Tf₂N] are very similar to the corresponding values in [hmim][Tf₂N].^{6,7} In both ionic liquids, the molar solution Gibbs energy becomes higher by a factor of about 2.6 when carbon dioxide is replaced by hydrogen. The gas exchange, however, turns the molar solution enthalpy from a negative value for carbon dioxide, which is typical for an exothermal process, into a positive value for hydrogen. The corresponding molar solution entropy is negative for both gases, and the absolute value is higher for carbon dioxide with a difference of about 53 % compared with hydrogen.

Conclusions

We report experimental results for the solubility of the single gases carbon dioxide and hydrogen in the ionic liquid [bmpy][Tf₂N] from about (293 to 413) K and up to approximately 10 MPa. Henry's law constants were determined from experimental solubility data, and solution thermodynamic properties for these two binary systems were in turn determined from Henry's law constants and discussed with the results from prior studies on different ionic liquids. Furthermore, the new experimental data for the gas solubility (i.e., the gas molality at given temperature and pressure) were correlated by an extension of Henry's law with an average relative deviation of about 0.8 % for the system (carbon dioxide + [bmpy][Tf₂N]) and of about 1.3 % for the system (hydrogen + [bmpy][Tf₂N]).

Acknowledgment

The authors thank Dr. K. Massonne, BASF SE, Ludwigshafen, Germany, for generously purchasing the ionic liquid [bmpy][Tf₂N] for our studies.

Literature Cited

- Anthony, J. L.; Anderson, J. L.; Maginn, E. J.; Brennecke, J. F. Anion effects on gas solubility in ionic liquids. *J. Phys. Chem. B* **2005**, *109*, 6366–6374.
- Jacquemin, J.; Husson, P.; Majer, V.; Costa Gomes, M. F. Influence of the cation on the solubility of CO₂ and H₂ in ionic liquids based on the bis(trifluoromethylsulfonyl)imide anion. *J. Solution Chem.* **2007**, *36*, 967–979.
- Hong, G.; Jacquemin, J.; Deetlefs, M.; Hardacre, C.; Husson, P.; Costa Gomes, M. F. Solubility of carbon dioxide and ethane in three ionic liquids based on the bis(trifluoromethylsulfonyl)imide anion. *Fluid Phase Equilib.* **2007**, *257*, 27–34.
- Hou, Y.; Baltus, R. E. Experimental measurement of the solubility and diffusivity of CO₂ in room-temperature ionic liquids using a transient thin-liquid-film method. *Ind. Eng. Chem. Res.* **2007**, *46*, 8166–8175.
- Aki, S. N. V. K.; Mellein, B. R.; Saurer, E. M.; Brennecke, J. F. High-pressure phase behavior of carbon dioxide with imidazolium-based ionic liquids. *J. Phys. Chem. B* **2004**, *108*, 20355–20365.
- Kumelan, J.; Pérez-Salado Kamps, Á.; Tuma, D.; Maurer, G. Solubility of CO₂ in the ionic liquid [hmim][Tf₂N]. *J. Chem. Thermodyn.* **2006**, *38*, 1396–1401.
- Kumelan, J.; Pérez-Salado Kamps, Á.; Tuma, D.; Maurer, G. Solubility of H₂ in the ionic liquid [hmim][Tf₂N]. *J. Chem. Eng. Data* **2006**, *51*, 1364–1367.
- Kumelan, J.; Pérez-Salado Kamps, Á.; Tuma, D.; Maurer, G. Solubility of the single gases methane and xenon in the ionic liquid [hmim][Tf₂N]. *Ind. Eng. Chem. Res.* **2007**, *46*, 8236–8240.
- Kumelan, J.; Pérez-Salado Kamps, Á.; Tuma, D.; Yokozeki, A.; Shiflett, M. B.; Maurer, G. Solubility of tetrafluoromethane in the ionic liquid [hmim][Tf₂N]. *J. Phys. Chem. B* **2008**, *112*, 3040–3047.
- Kumelan, J.; Pérez-Salado Kamps, Á.; Tuma, D.; Maurer, G. Solubility of the single gases carbon monoxide and oxygen in the ionic liquid [hmim][Tf₂N]. *J. Chem. Eng. Data* **2009**, *54*, 966–971.
- Maurer, G.; Pérez-Salado Kamps, Á. Solubility of gases in ionic liquids, aqueous solutions, and mixed solvents. In *Developments and Applications in Solubility*; Letcher, T., Ed.; RSC Publishing: Cambridge, 2006; pp 41–58.
- Wagner, W.; Overhoff, U. *ThermoFluids Version 1.0 (Build 1.0.0)*; Springer Verlag: Berlin, Heidelberg, 2006.
- Hayden, J. G.; O'Connell, J. P. A generalized method for predicting second virial coefficients. *Ind. Eng. Chem., Process Des. Dev.* **1975**, *14*, 209–216.
- Span, R.; Wagner, W. A new equation of state for carbon dioxide covering the fluid region from the triple-point temperature to 1100 K at pressures up to 800 MPa. *J. Phys. Chem. Ref. Data* **1996**, *25*, 1509–1596.
- Pérez-Salado Kamps, Á.; Tuma, D.; Xia, J.; Maurer, G. Solubility of CO₂ in the ionic liquid [bmim][PF₆]. *J. Chem. Eng. Data* **2003**, *48*, 746–749.
- Kumelan, J.; Pérez-Salado Kamps, Á.; Tuma, D.; Maurer, G. Solubility of CO₂ in the ionic liquids [bmim][CH₃SO₄] and [bmim][PF₆]. *J. Chem. Eng. Data* **2006**, *51*, 1802–1807.
- Kumelan, J.; Pérez-Salado Kamps, Á.; Tuma, D.; Maurer, G. Solubility of the single gases H₂ and CO in the ionic liquid [bmim][CH₃SO₄]. *Fluid Phase Equilib.* **2007**, *260*, 3–8.
- Kumelan, J.; Pérez-Salado Kamps, Á.; Tuma, D.; Maurer, G. Solubility of H₂ in the ionic liquid [bmim][PF₆]. *J. Chem. Eng. Data* **2006**, *51*, 11–14.
- Zaitsau, Dz. H.; Kabo, G. J.; Strechan, A. A.; Paulechka, Ya. U.; Tschersich, A.; Verevkin, S. P.; Heintz, A. Experimental vapor pressures of 1-alkyl-3-methylimidazolium bis(trifluoromethylsulfonyl)imides and a correlation scheme for estimation of vaporization enthalpies of ionic liquids. *J. Phys. Chem. A* **2006**, *110*, 7303–7306.
- Pitzer, K. S. Thermodynamics of electrolytes. 1. Theoretical basis and general equations. *J. Phys. Chem.* **1973**, *77*, 268–277.
- Pitzer, K. S. Ion interaction approach: theory and data correlation. In *Activity Coefficients in Electrolyte Solutions*; Pitzer, K. S., Ed.; CRC Press: Boca Raton, FL, 1991; pp 75–155.
- Kumelan, J.; Tuma, D.; Maurer, G. Partial molar volumes of selected gases in some ionic liquids. *Fluid Phase Equilib.* **2009**, *275*, 132–144.
- Dyson, P. J.; Laurenczy, G.; Ohlin, C. A.; Vallance, J.; Welton, T. Determination of hydrogen concentration in ionic liquids and the effect (or lack of) on rates of hydrogenation. *Chem. Commun.* **2003**, 2418–2419.

Received for review March 25, 2009. Accepted May 26, 2009. The authors appreciate financial support by Deutsche Forschungsgemeinschaft (DFG), Bonn-Bad Godesberg, Germany.

JE900298E